

# WHAT IS THE PHYSICS OF PULSAR RADIO EMISSION?

A white paper submitted to the  
Astro2010 Science Frontier Panel  
*Stars and Stellar Evolution*

T. H. Hankins  
(575) 835-7326  
New Mexico Institute of Mining and Technology  
thankins@aoc.nrao.edu

J. M. Rankin  
(802) 656-0051  
University of Vermont  
joanna.rankin@uvm.edu

J. A. Eilek  
(575) 835-7393  
New Mexico Institute of Mining and Technology  
jeilek@aoc.nrao.edu

February 15, 2009

# What is the Physics of Pulsar Radio Emission?

T. H. Hankins, J. M. Rankin, and J. A. Eilek

Pulsars provide a clear case of coherent radio emission from outside the Solar System. Despite much careful theoretical and observational effort, the details of how these rapidly rotating neutron stars radiate are still a mystery. In this paper we focus on this important issue, which has remained unsolved since pulsars were discovered: **how can we understand the physics of the coherent radio emission from pulsars?**

Pulsars are dramatic laboratories for extreme physics. It is thought that the radio-loud regions in pulsar’s magnetosphere are ruled by plasma electrodynamics in a rotating system. The magnetic field is strong enough for quantum effects to matter, such as pair creation and quantized gyromotion. The induced electric field is strong enough to accelerate charges to very high Lorentz factors. A relativistic plasma within this system emits coherent radiation as a by-product of plasma dynamics, strong turbulence and pair creation. Although this hypothesis has gained wide acceptance, **it must be tested by measurements using the widest possible bandwidths, the highest possible time resolution and the best possible sensitivity.**

Theoretical models of pulsar radio emission have proliferated virtually unchallenged because they are hard to test with traditional pulsar observations. In this paper we identify new measurements which can reveal physical conditions in the emission region, or test competing theoretical models of that region.

What measurements can best address the underlying emission physics? Ultra-wide bandwidth, ultra-high time resolution observations are critical, because *models diverge in what they predict for short time scales and fundamental emitter bandwidths*. The emission changes within one rotation period, so we must have the *highest possible sensitivity* data to see individual “pulses”. We need radio observations which can resolve the *dynamic time-scales of the plasma* (on the order of  $10^{-7}$  to  $10^{-5}$  s), the *intrinsic plasma-turbulent time scales* (as short as  $10^{-9}$  s), and reveal the intrinsic bandwidths of the emission.

Polarization measurements at high time resolution are a critical component of every approach to understanding pulsar radiation. Wave polarization provides almost

all information about the emission geometry and reflects the physics of the emission and/or propagation directly. High sensitivity is absolutely key because useful polarimetry requires that the received signal level  $S$  substantially exceed the noise level  $N$ , *e.g.*,  $S/N \gg 1$ .

## The basic picture of pulsars and its limitations

A “standard model” of a pulsar’s magnetosphere has been developed from observational evidence and theoretical considerations [3, 13]. A rapidly rotating neutron star supports a misaligned, dipolar magnetic field. The plasma-filled magnetosphere corotates with the star except in the open field line region where the star’s magnetic poles connect to the universe past the light cylinder.<sup>1</sup> We call this open field line region the polar flux tube (PFT). Plasma in the PFT emits coherent radio emission, which we observe as “pulses” when the star’s rotation

---

<sup>1</sup>The radial distance from the pulsar’s rotation axis which would co-rotate with the pulsar at the speed of light.

Focus:	Emission region	Plasma dynamics	Plasma emission
Time:	milliseconds	microseconds	nanoseconds
Size scales:	⇒ polar flux tube	⇒ ~ 1 km	⇒ ~ 1 m
Observational tests:	Mean profile, subpulse drift and polarimetry	Intensity, polarization of microstructure	Intensity nanostructure, dynamic spectra

Table 1: Relationship of the time scales, physical picture, and observations for understanding the physics of the pulsar radio-loud regions.

sweeps this region past our line of sight.

While this picture is generally accepted and probably close to correct, there remain important, unresolved observational and theoretical issues.

**Unresolved issues: Phenomenology.** A general picture of the emission region geometry has emerged from observations. Radio emission is thought to originate at moderate altitudes in the PFT (several tens of stellar radii), well within the light cylinder. The radio-loud plasma in the PFT is strongly constrained by the dipolar magnetic field, and is usually confined to a conal distribution (located around the edge of the PFT) or a coral one (located centrally within the PFT). If the star’s magnetic axis is strongly tilted relative to its rotation axis, both magnetic poles may be visible, creating both a main pulse and interpulse, as in the Crab pulsar. However, some significant results do not easily fit this picture.

One such result is **time variability**. We divide the time scales relevant to the physics of pulsar emission into three areas as summarized in Table 1. The geometrical picture of the PFT derives from *mean profiles*, which describe pulsar emission synchronously averaged over many rotation periods. But the radio emission is far from steady when studied at high time resolution. Analysis of sequential pulse periods has shown that some pulsars have accurately drifting *subpulses* which are consistent with a rotating subbeam “carousel” of emitters distributed around the emission cone and having a loca-

tion “memory” or “history” that survives for many stellar rotation periods. An example is shown in Figure 1. The “carousel” sub-

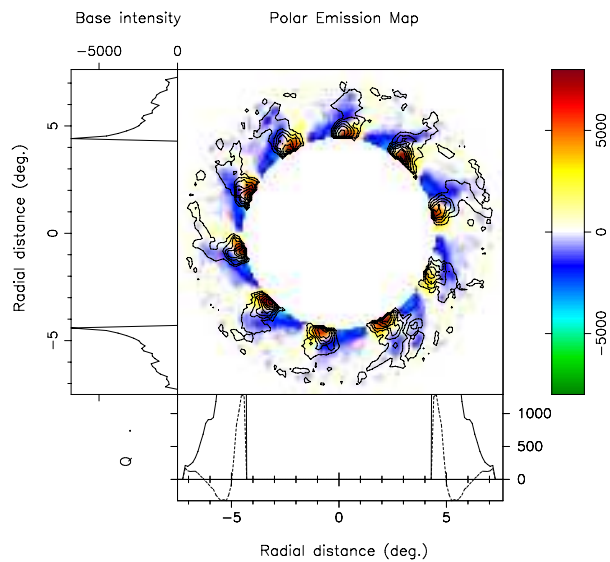


Figure 1: Composite 10-subbeam map of pulsar B0809+74 in total and total-linear power at 328-MHz from [12]. The contours show the total power beam-system intensities with the circularly symmetric “base” function subtracted. The color-intensity coding gives the respective linear polarization according to the scale at the right of the diagrams. The aggregate intensity in the two orthogonal polarization modes is distinguished only by its sign: the positive (yellow-orange) modal “beamlets” are more intense and fall inside of the polar emission pattern; whereas the negative (blue-cyan-green) beamlets occur further from the magnetic axis, fall off in a canted manner and are generally weaker. Here the sightline cuts across the polar-cap emission pattern from right to left at the bottom of the diagram. The total power (solid curve) and residual linear (dotted) radial beam forms are shown in the bottom panel.

beam rotation is thought to be driven by an  $\mathbf{E} \times \mathbf{B}$  drift in the PFT [13], which provides an observable quantity related to the  $\mathbf{E}$  and  $\mathbf{B}$  fields about the polar cap.

*Microstructure* (less-ordered intensity variations with time-scales 1 to 500 microseconds) is seen in nearly all bright pulsars, but no consensus has been reached as to its origins. An example of microstructure in the Crab pulsar is shown in the next section as Figure 3. We suspect that microstructure is tied to plasma dynamics within the emission region.

In Figure 4 we show that even finer-scale temporal structure exists; *nanostructure* has been detected in the Crab pulsar (distinct bursts unresolved at  $\Delta t = 0.4$  nanoseconds [5]). The associated length scales,  $c\Delta t$ , are less than 1 m, suggesting that we are seeing the individual emitting “entities”.

Another significant observable is **polarization**. Linearly polarized radio emission in a rotating dipolar field leads to a characteristic rotation of position angle, seen in many pulsars, *but not all*. Some stars show time-steady position angle rotations which are not consistent with a dipole field. Other stars show highly variable position angle fluctuations within a single pulse, which we suspect reveals the underlying plasma dynamics.

Many issues related to polarimetry remain unanswered, and have the potential to be used as probes of the emission physics. What determines the linear and circular polarization of a signal? What causes the rapid orthogonal mode transitions in linear polarization, and the rapid sign changes of circular polarization? Are these a signature of the emission process, or a result of propagation in the pulsar’s magnetosphere? Why does Crab nanostructure polarization fluctuate wildly, as in Figure 4, whereas for a few slow pulsars it is constant across a micropulse? Recent work demonstrates that many pulsars retain a natal supernova alignment between their proper-motion and rotation-axis direc-

tions [6, 7, 11]. This development opens the possibility that the linear polarization direction can be related to the projected magnetic field direction and thus interpreted physically for the first time.

**Unresolved Issues: Physics.** The generally accepted pulsar model combines the observationally-motivated geometry with basic electrodynamics of rotating, magnetized neutron stars. Charged particles from the star’s surface are accelerated by strong  $\mathbf{E}$  fields which exist close to the star in a “gap” region. As the particles follow the  $\mathbf{B}$  field lines they emit  $\gamma$ -ray photons, which produce electron-positron pairs in the strong  $\mathbf{B}$  field. Further  $\gamma$ -ray production by the daughter leptons initiates a pair production cascade, which terminates the “gap” region by creating a dense pair plasma which shields the accelerating  $\mathbf{E}$  field. Above the gap region, the plasma is coasting, still at relativistic speeds; this plasma is believed to emit coherent radio pulses. However, *some significant theoretical issues remain unresolved within this picture.*

One such issue is **the dynamical state** of the radio-loud plasma. Smooth plasma flow in the PFT is an essential element of the standard model. This requires that the plasma have a particular value of the charge density (the “Goldreich-Julian”, or GJ, density [3]), so that the rotation-induced  $\mathbf{E}$  field is fully shielded. There are, however, several complications:

- An oblique rotator cannot support static plasma corotation at any density [1].
- The pair cascade does not necessarily produce the GJ charge density [2].
- The identification of Strong Plasma Turbulence as the emission mechanism in the Crab pulsar [4] requires the local charge density to be far below the GJ value. Therefore it is very likely that the plasma in the emission region is highly unsteady; *we suspect that microstructure is the observational signature of this nonsteady plasma.*

Another issue is **the nature of the coherent radio emission**. It is likely that the free energy in the plasma current flow converts to radiation through an instability, but how this works has been unclear. Three types of radio emission models have been proposed, *e.g.*, [10], and their timescales are compared in Table 2.

- In *plasma turbulence* models, plasma wave energy is converted into escaping radiation by modulational processes and 3D soliton collapse.

- In the *coherent curvature* model, curvature emission is enhanced by the bunching of charges either in streaming-unstable waves or in 1D electrostatic solitary waves. High brightness in these two types of models is due to spatial coherence.

- *Maser-like* mechanisms produce stimulated emission of radiation through various phase-coherent means, such as Čerenkov emission or Compton scattering.

Emission Process	Saturation Mechanism	Saturation Timescale
plasma turbulence	soliton collapse	$\lesssim 1$ ns
coherent curvature	beam trapping	0.01 to 1 $\mu$ s
maser	quasilinear diffusion	0.1 $\mu$ s

Table 2: Predicted variability of some emission processes that have been proposed. The plasma turbulent timescales come from numerical simulations [14] shown in Figure 2. The other timescales are analytical estimates of the physical processes.

## What needs to be done?

What can be measured that will probe the physics of the radio loud region, the physics of the radio emission, and the environmental constraints on these processes? We believe

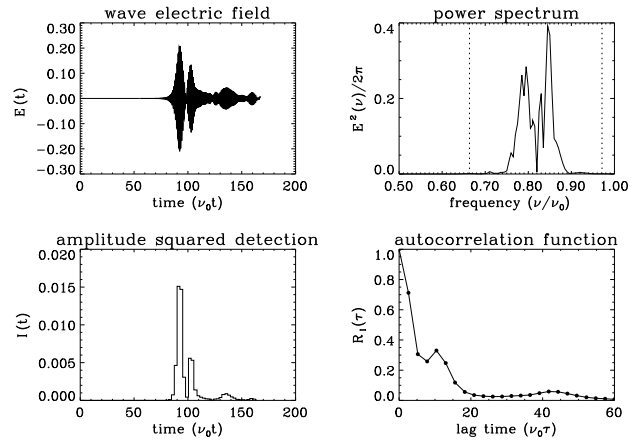


Figure 2: Results of the Strong Plasma Turbulence simulation from [14]. The electric field created by a collapsing soliton is computed as a function of time, scaled to 5 GHz as the observation frequency. The time structure is characteristic of nanopulses or “shots” in the strong turbulence model, and comes from modulational coupling with the electrostatic pump wave. Time units are in cycles of the plasma frequency,  $\nu_0$ .

that the keys to the pulsar puzzle lie in a critical understanding of the emission region geometry, and comparing high time resolution measurements of individual pulses and precision, high-sensitivity polarimetry with quantitative theoretical predictions which can be tested against the data.

### First case study: The Crab pulsar

A start on this work has been made by high time resolution observations of the Crab Nebula pulsar. For example, consider the competing radio emission models described above. Simple estimates of the timescales for each of the models (summarized in Table 2) show that the three mechanisms predict quite different timescales, which can be distinguished by high time resolution observations.

Careful numerical modeling [14] of Strong Plasma Turbulence reveals explosive spatial collapse of regions of high electric field (“solitons”) and consequent bursts of radi-

tion as shown in Figure 2. These solutions show that the functional form of an individual “shot” impulse can be derived from the source physics. The emission bandwidth,  $\Delta\nu/\nu \sim 0.2$ , is centered on the co-moving plasma frequency; there is a distinctive time signature due to coupling of the electromagnetic modes to the turbulence:  $\nu\Delta t \sim O(10)$ . Thus, observations at 5 GHz should reveal  $\Delta t \sim 1 - 2$  ns and shorter at 9 GHz. *These predictions have been confirmed in observations of the Crab pulsar* [4, 5]. In Figure 3 we show 20% wideband emission and microstructure from the Crab and in Figure 4 we show unresolved nanopulses.

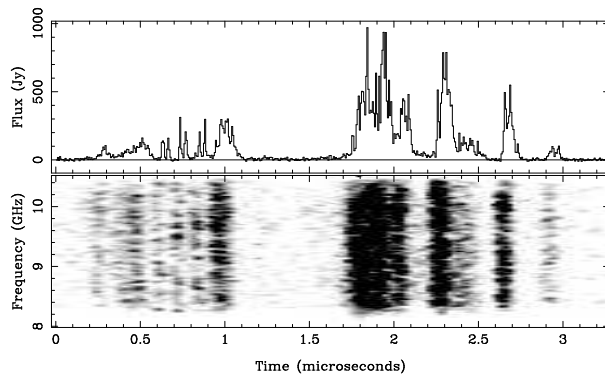


Figure 3: A single Crab Main Pulse shown here was recorded over a 2.5-GHz bandwidth centered at 9.25 GHz at Arecibo [5]. The flux is plotted with 8-ns time resolution. The dynamic spectrum shows that the total emission is relatively wideband.

**Magnetospheric propagation.** There are at least two issues concerned with propagation in the pulsar magnetosphere, the settlement of which require much more sensitive and wideband observations as well as interpretation.

*Magnetospheric turbulence.* Measurements of the Crab Nebula pulsar’s “giant pulses” show that the width,  $w$ , of the main pulse micropulse components scale with frequency,  $\nu$ , as  $w \propto \nu^{-2}$  [8]. If this results from propagation through turbulence, then

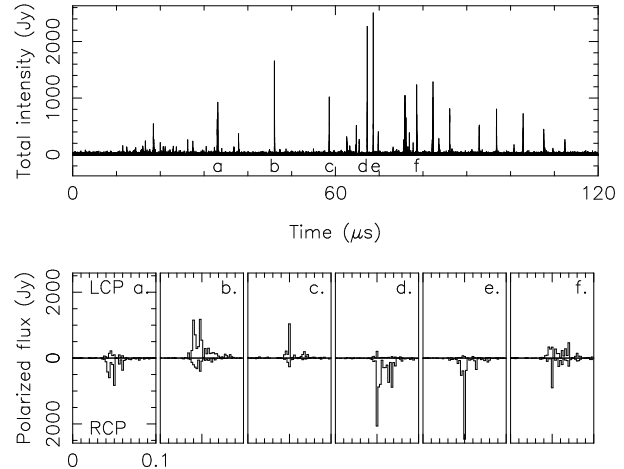


Figure 4: The intensity, polarization and time structure of nanopulses in the Crab pulsar recorded at the Arecibo Observatory at 5 GHz are shown [4]. The upper panel shows the whole pulse; sections of 100-ns duration showing the polarized flux from six of the nanopulses labeled a to f, are plotted below with 2-ns resolution; left circular polarization upward and right circular polarization downward.

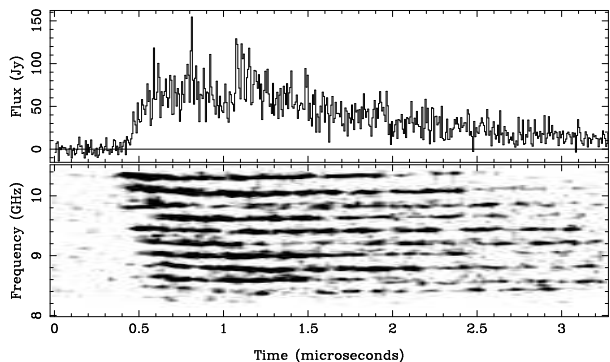


Figure 5: An interpulse from the Crab pulsar, recorded four minutes after the main pulse shown in Figure 3 and processed in exactly the same way, with the same time and frequency scales. The banded frequency structure occurs in *every* IP recorded above 5 GHz. The separation  $\Delta\nu$  of the band center frequencies is approximately  $\Delta\nu = 0.06\nu$  over the frequency range  $5 \leq \nu \leq 10$  GHz. The onset of the pulse in the dynamic spectrum is frequency dependent, which implies that the IP has a slightly higher dispersion than the MP.

the turbulent structures are not Kolmogorov, which predicts temporal broadening  $w \propto \nu^{-4.4}$ , as seen in the interstellar medium. To test other pulsars for this phenomenon high sensitivity and wide bandwidths are required.

*Interpulse emission.* By comparing Figures 3 and 5 it is clearly seen that the dynamic spectrum of the Crab interpulse emission is dramatically different from that of the main pulse. Although several models have been proposed, testing them requires measurements on other pulsars. Does the banded structure of the Crab interpulse dynamic spectrum result from emission conditions or propagation in the magnetosphere? At frequencies high enough to avoid contamination by interstellar scattering propagation effects, even the main pulse emission of other pulsars is weak, so wide bandwidths and high sensitivity are required to test the proposed hypotheses.

## Where to Go Next

The extremely bright “giant pulses” emitted by the Crab pulsar have provided an excellent base for radio emission measure studies. The detection of isolated nanoshots in the Main Pulse of the Crab pulsar [5] is consistent with only one of the current emission models, namely coherent emission from strong plasma turbulence. But other stars *must* be tested for nanostructure; we have no guarantee that the Crab pulsar is not unique, and one might argue that conclusions based on its study are not applicable to other stars. The Crab giant pulses in which nanoshots have been detected are *far* more intense than even the brightest of other pulsars. Consequently, the utmost sensitivity for testing these hypotheses is necessary, as afforded only by the 1000-foot Arecibo radio telescope and the future Square Kilometer Array.

**Nanostructure and emission bandwidths.** A key observational test for the

Strong Plasma Turbulence model is the bandwidth  $\Delta\nu/\nu \leq 0.2$  predicted for the emission from soliton collapse. This test requires larger bandwidths than are currently available at the largest radio telescopes. Furthermore, large bandwidths are required to separate intrinsic frequency structure from that imposed by propagation through the inhomogeneous interstellar medium, *i.e.*, interstellar scattering. New technology in the form of low-noise decade-bandwidth dual-polarization antenna feeds and associated low-noise amplifiers are required as well as data recording systems fast enough to sample these bandwidths. Such technological developments are in progress for SETI and other projects; fast analog to digital converters and recording systems by the commercial sector (*e.g.*, Teledyne Scientific, E2N, National Semiconductor). In the design and construction of the SKA these requirements should be considered, though *it is technically far simpler to augment and support existing single-dish telescopes like Arecibo with wide-band feeds and fast recording devices.*

**Polarimetry.** Resolution of single pulses to the microstructure level with full Stokes polarization is required to advance our understanding of the pulsar radio emission mechanism and the propagation of the radio emission through the pulsar magnetosphere. Although calibration techniques for accurate polarimetry are now well known, attention must be paid to the polarization characteristics of new wideband feed systems to assure that they can be accurately and unambiguously calibrated. To take advantage of these wide bands we will need fast digital “backend” data acquisition systems with high dynamic range to allow interference excision without corrupting pulsar signals in interference-free bands.

## Summary

Pulsars provide the only place accessible to observations where quantum-strong  $\mathbf{E}$  and  $\mathbf{B}$  fields exist. The challenge of understanding the physics in these regions can be met. Critical tests of theoretical coherent radio emission models require the highest possible bandwidths, the shortest time resolution afforded by these bandwidths, and the best possible sensitivity afforded by the largest radio telescopes.

## References

- [1] Arendt, P.N., Jr. 2002, *Ph.D. Thesis*, New Mexico Institute of Mining and Technology
- [2] Arendt, P.N. Jr. & Eilek, J.A. 2002, *ApJ*, **581**, 451
- [3] Goldreich, P. & Julian, W.H. 1969, *ApJ*, **157**, 869
- [4] Hankins, T.H., Kern, J.S., Weatherall, J.C. & Eilek, J.A. 2003, *Nature*, **422**, 141
- [5] Hankins, T.H. & Eilek, J.E. 2007, *ApJ*, **670**, 693
- [6] Johnston, S., Hobbs, G., Vigeland, S. Kramer, M., Weisberg, J.M. & Lyne, A.G. 2006, *ChJAS*, **6**, 237
- [7] Johnston, S., Kramer, M., Karastergiou, A., Hobbs, G., Ord, S. & Wallman, J. 2007, *MNRAS*, **381**, 1625
- [8] Kern, J., 2004, *Ph.D. Thesis*, New Mexico Institute of Mining and Technology
- [9] Luo, Q. & Melrose, D.B. 1995, *MNRAS*, **276**, 372
- [10] Melrose, D.B. 1992, in *Proc. IAU Colloq No. 128*, 307
- [11] Rankin, J.M. 2007, *ApJ*, **664**, 443
- [12] Rankin, J.M. Ramachandran, R., van Leeuwen, J. Suleymanova, S.A. 2006, *A&A*, **455**, 215
- [13] Ruderman, M.A. & Sutherland, P.G. 1975, *ApJ*, **196**, 51
- [14] Weatherall, J.C. 1998, *ApJ*, **506**, 341